INTERNATIONAL JOURNAL OF ENVIRONMENTAL ANALYTICAL CHEMISTRY
2024, VOL. 104, NO. 20, 9632–9651
https://doi.org/10.1080/03067319.2023.2240718

Adsorption behavior of reactive Red 24 and methylene blue onto Brewer's spent grain: characterization, kinetics, and isotherms modeling

Çiğdem Ay[a], Şaziye Betül Sopaci[b], Orhan Atakol[c] and Sevi Öz[d]

[a]Faculty of Science and Art, Department of Chemistry, Kütahya Dumlupınar University, Kütahya, Turkey; [b]Faculty of Science and Art, Department of Chemistry, Kırşehir Ahi Evran University, Kırşehir, Turkey; [c]Faculty of Science, Department of Chemistry, Ankara University, Ankara, Turkey; [d]Polatlı Faculty of Science and Art, Department of Chemistry, Ankara Hacı Bayram Veli University, Ankara, Turkey

ABSTRACT

Dyestuff wastes, made by the textile, paper, and dye industries, stay in the waste environment because they resist chemical and biological degradation. Treating industrial effluent to remove pollutants and lessen their effects before releasing them into the environment is crucial. Malt bagasse (BSG; Brewer's Spent Grain) from a local brewery was used as an adsorbent for the textile industry dyes Methylene Blue (MB) and Reactive Red 24 (RR24). The adsorption of MB and RR24 was conducted at pH 7.00 and 1.50, respectively. While the temperature change had little effect on the MB adsorption process and capacity, the RR24 adsorption rate was increased without affecting the capacity. Both dyes' adsorption mechanisms better fit the Langmuir isotherm and pseudo-second-order kinetic models. The maximum adsorption capacity was 80.31 mg/g for MB and 100.52 mg/g for RR24. Experiments using simulated wastewater indicated that the matrix did not significantly affect the efficiency with which RR24 and MB were removed. The findings suggest that BSG is a promising alternative adsorbent that is inexpensive, accessible, and simple to obtain.

ARTICLE HISTORY
Received 30 May 2023
Accepted 20 July 2023

KEYWORDS
Adsorption; Brewer's Spent Grain; Malt Bagasse; Methylene Blue; Reactive Red 24

1. Introduction

Pollution and pollution loads in natural resources are increasing daily as the industry develops. Notably, the dyeing process in the textile industry creates a lot of water waste, which is a significant source of pollution. Worldwide, various industries use close to 10,000 dyes to colour their products, and their annual production exceeds 7×10^6 tons [1]. Azo dyes, one of the oldest industrially synthesised dye types, account for 60–70% of yearly production worldwide. Reactive dyes, one of the azo dyestuffs, are preferred in the textile industry due to their attractive properties, such as easy application, high photolytic stability, availability of a wide variety of bright tones, strong covalent adhesion to textile fibres, and minimum energy requirement [2]. Approximately 10–15% of the annual dye consumption in the textile industry is discharged as waste [3–5]. Dyeing in the textile industry involves using numerous complex organic and inorganic chemicals [6]. In

CONTACT Çiğdem Ay cigdem.ay@dpu.edu.tr

particular, dyestuffs with high water solubility contribute significantly to wastewater problems. Also, because they are made of large molecules of organic matter, they strongly raise water's biological oxygen demand (BOD) value. In other words, the high water solubility of dyestuffs is a significant cause of water pollution, as it not only increases the volume of pollutants in the water but also uses up oxygen necessary for aquatic organisms to survive. Mixing water pollution with soil alters the soil's biological properties and poses a threat to human health by entering the food chain [7,8]. For instance, a dye concentration of 1.0 mg/L in drinking water is toxic to human health, and verifying the quality of the water is vital. In addition, the toxicity can cause severe harm to humans, including dysfunction of the kidneys, reproductive system, liver, brain, and central nervous system [7,9–11]. It is estimated that 80% of all infectious diseases in the world are linked to contaminated water and that 3,4 million people, primarily children, pass away each year from water pollution [12–15]. As a result, many countries have enacted stringent regulations regarding chemicals in water, requiring industries to properly treat industrial effluents before discharging them into natural waterbodies containing clean water [16]. Although there are many techniques for removing pollutants from wastewater, such as coagulation, chemical oxidation, membrane separation, and aerobic/anaerobic microbial degradation, these methods have yet to be successful because of various limitations, such as high costs, inefficiency at low concentrations, time-consuming processes, and chemical sludge [17–19]. Adsorption has been accepted as an efficient and effective method for dye removal due to its low cost, simplicity, ease of regeneration, no sludge, and lack of toxic intermediate products. During the adsorption process, the adsorbent can be regenerated, stored in a moisture-free environment, and reused in processes that do not require high-purity water [20–22]. Due to its economy and environmental friendliness, many adsorbents, such as activated carbon [23], zeolite [24], agro-waste [25], clays [26], and plant fibres [27], are used in adsorption processes. As low-cost adsorbents under different operating conditions, several agro-wastes (fruit peels, plant leaf/root/stem/seed, factory fruit, and vegetable waste) be used to remove various dyes. Using factory waste as an adsorbent is very economical and effective in removing dyes from wastewater. The phenomenon not only helps reduce the cost of waste disposal but also provides a sustainable solution for treating wastewater. Additionally, using factory wastes as adsorbents can be a step towards achieving a circular economy.

The production of beer is a dynamic industry with a critical key economic and strategic role in the food sector. According to the report prepared by the Turkish Agricultural Economy and Policy Development Institute, the production of beer barley in 2021 has been reported at 250 thousand tons [28]. As per data from 2020, beer, the fifth most consumed beverage in the world, is also the most consumed alcoholic beverage [29]. Spent grain is the largest amount of waste in the brewery industry, accounting for about 85% of brewery waste [30]. Brewers' spent grain (BSG), which is the main by-product of the brewing industry, with a global production of 39 million tons per year, is a lignocellulosic material with a fibre content of up to 70%, including cellulose (16–25%), hemicellulose (28–35%), and lignin (7–27%), and protein content of 25–30% [31,32]. Also, BSG consists of hydroxyl, carboxyl, and various functional groups used as active binding sites for adsorption [33]. BSG varies depending on the conditions used in malt production and mashing and the additives used in beer production, such as corn and rice [34].

Therefore, in this study, BSG obtained from a brewery in our country was used as an adsorbent without pretreatment. Given the huge amount of BSG produced on a continuous basis, it remains appealing to investigate alternative approaches that require less energy, less toxic chemicals, and simpler processes to recycle BSG as an effective adsorbent and improve its application potential [35].

The adsorption interest of BSG on both reactive and basic dyes was examined in this work using reactive red 24 (RR24) and methylene blue (MB) dyes, which are extensively utilised in the textile industry and many other sectors. The kinetic and isotherm parameters of adsorption were calculated using experimental data obtained from batch system experiments. In addition to these studies, characterisation of the adsorbent was performed, and the findings have paved the way for increased adsorbent capacity. Also, the research can help design cost-effective and eco-friendly methods for removing dyes from wastewater. Further research can be conducted to explore the potential of BSG as an alternative adsorbent for other pollutants present in wastewater.

2. Materials and methods

2.1. Preparation of BSG and dye solutions

The spent grains were obtained from Anadolu Efes Brewing and Malt Industry (Kahramankazan, Turkey). BSG without any pretreatment and at 85% humidity was dried at 60°C for 24 hours. BSG sieved through a 150 µm sieve, was dried at 60°C for 2 hours and used for adsorption studies. Stock solutions of dyes were prepared separately by dissolving the correct amount of RR24 ($C_{26}H_{17}ClN_7Na_3O_{10}S_3$, molar weight of 788.1 g/mol, λ_{max} in 534 nm) and MB ($C_{16}H_{18}ClN_3S$ molar weight of 319.9 g/mol, λ_{max} in 662 nm) in deionised water. MB was obtained from Merck (CAS No 122965-43-9) and RR24 (CAS No. 70210-20-7) from Kimetsan and used directly without purification. The chemical structures of dyes are shown in Figure 1(a,b). Solutions in the various concentrations were prepared from the stock solutions of dyes.

2.2. Characterization of BSG

Fourier Transform Infrared Spectroscopy (FT-IR) analyses were used to identify the active functional groups on the malt cake's surface. Furthermore, malt samples after dye adsorption were examined. 1/100 KBr tablets were prepared, and the samples were analysed with a Shimadzu Infinity FT-IR spectrometer with a wavelength range of 600–4000 cm^{-1}, 4 cm^{-1} resolution, and 16 scans/sample. Thermogravimetric (Shimadzu DTG-60) measurements were taken with an aluminium pan (heating rate: 10°C/min; N_2 atmosphere). The BSG morphology was investigated by Field Emission Scanning Electron Microscope (FE-SEM QUANTA 400F, USA) with Energy-dispersive X-ray spectroscopy (EDX). To prevent electrostatic charge, BSG and dye-loaded BSG were attached to an adhesive carbon tape and coated with gold/palladium.

Samples solutions in 50.0 mL NaCl (0.01 M) at different pH (1 to 10) and 0.150 g BSG were used to determine the point zero charge (pH_{pcz}) The samples were mixed at room temperature for 24 hours. Following this period, the final pH was determined, and data for pH_{pcz} determination were plotted [36].

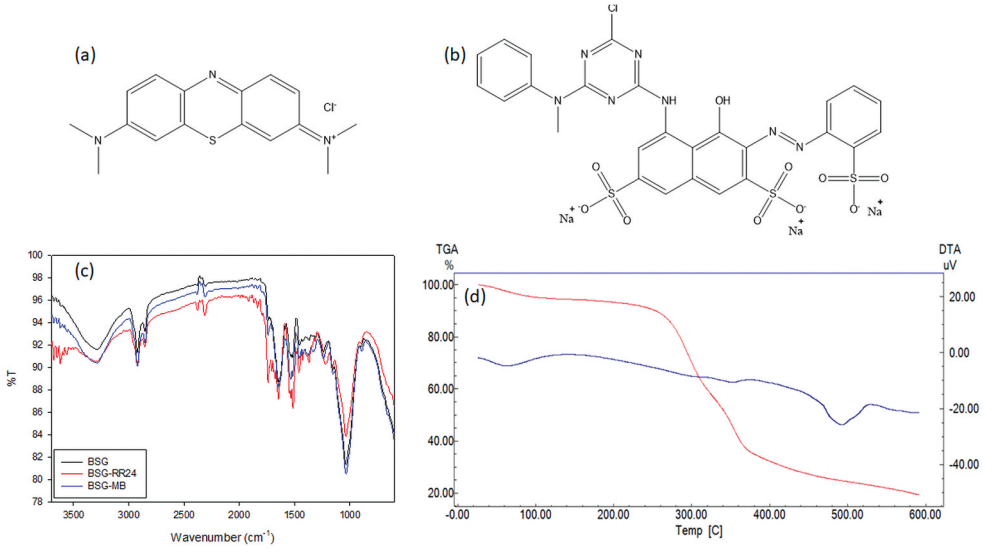

Figure 1. The chemical structures of MB (a) and RR24 (b); FT-IR Spectra (c) and TGA-DTA pattern (d) of BSG.

2.3. Adsorption experiments

The effects of adsorbent dosage, pH, contact time, temperature, and ionic strength on the adsorption performance of BSG were studied using batch adsorption tests.The experiments were conducted with BSG in an erlenmeyer on a multi-magnetic stirrer (IKA, RO 15) to determine the optimum pH where the maximum adsorption was accomplished for RR24 and MB. The pH experiments were carried out by mixing 0.025 g of dry-weight of adsorbent with 50.0 mL of 25 mg/L of dyes at 20°C. The pH of the solution was initially adjusted by adding a small amount of HCl or NaOH and measured using a pH meter (Hannah, HI 221). Also, experiments with adsorbent dosages ranging from 0.01–0.20 g were performed at room temperature with a dye concentration of 100 mg/L (for RR24) and 25 mg/L (for MB) at determined pH values. 100 mg/L of dyes solution containing NaCl and KCl at various concentrations (0.02–0.5 M) were prepared to examine the effect of ionic strength on the RR24 and MB adsorption performance of BSG. After the adsorbent was filtered off, the amount of RR24 and MB remaining in the solution was determined by a UV-vis spectrophotometer. Kinetic and isotherm experiments were carried out at different temperatures (20°C, 30°C, 40°C, and 50°C) at the pH values determined for the adsorption of RR24/MB onto BSG. Kinetic studies were conducted with 3 g/L BSG at a dye concentration of 100 mg/L, whereas isotherm experiments were conducted with 0.150 g BSG in 50.0 mL over the concentration range of 50–500 mg/L dyes.

Under optimum adsorption conditions, regeneration studies were conducted to evaluate the adsorbent's ability of repetitive use in the removal of RR24 and MB. Adsorption/desorption cycles were repeated five times with 0.1 M NaOH for RR24 and 0.1 M HCl for MB as regeneration solutions.

The adsorption capacity (q_e, mg/g) and adsorption yield (Removal %) of RR24 and MB were calculated as follows:

$$q_e = \frac{(C_0 - C_e)V}{m} \quad (1)$$

$$Removal\ \% = \frac{C_0 - C_e}{C_0} x100 \quad (2)$$

where C_o (mg/L) and C_e (mg/L) are the dye concentrations before and after adsorption, m (g) is the mass of BSG, and V (L) is the volume of dye solutions.

2.4. Application in synthetic wastewater

The synthetic wastewater medium listed in Table 1 was made to study wastewater constituents' impact on RR24 and MB adsorption [37]. 0.150 g of BSG was added to 50.0 mL of synthetic wastewater and mixed for one hour at 20°C at the appropriate pH for RR24 and MB. Then, the effect of synthetic wastewater on adsorption efficiency for both dyes was investigated.

3. Results and discussion

3.1. Characterization of adsorbent

3.1.1. FT-IR analysis

In Figure 1(c), FT-IR spectra of BSG before and after RR24/MB adsorption are given. Broad absorption bands at 3200–3400 cm^{-1} can be attributed to overlapping O – H and N – H stretching vibrations, which are prevalent in proteins and lignocellulose [31].

The antisymmetric and symmetric stretching vibrations of $-CH_2$ groups in cellulose and hemicellulose are attributed to the absorption bands at 2900 and 2800 cm^{-1}. In contrast, the absorption bands at 1240 and 1035 cm^{-1} are assigned to C–N and C–O–C stretching vibrations. The antisymmetric –COO– stretching vibration is associated with the absorption band located at 1643 cm^{-1} in the BSG spectrum. Protein-related bond overlap is also associated with this band (amide I groups). The absorption band in proteins found at 1529 cm^{-1} is associated with amide II groups. Also, the symmetrical stretching vibration of the –COO– groups can be observed at 1456 cm^{-1}. The most significant change with the adsorption of RR24 on BSG is the appearance of the signal observed at 1739 cm^{-1}. This signal undoubtedly indicates that the intensity of the C=O stretches is

Table 1. Composition of synthetic wastewater.

Components	g/L
Glucose	0.50
KH_2PO_4	0.30
$MgSO_4.7H_2O$	0.02
$CaCl_2.2H_2O$	0.10
Na_2SO_4	0.10
Na_2CO_3	0.20
$FeSO_4.7H_2O$	0.04
$NiCl_2.6H_2O$	0.02
$CuSO_4.5H_2O$	0.006
RR24/MB	0.025

increasing. While RR24 lacks a carbonyl group, the naphthalene ring does have –OH and N –H groups. As a result of hydrogen bonding or transfer of the -OH group in the naphthalene ring to the -N-H group, an o-quinoid structure can easily be formed in the naphthalene ring. Therefore, the change between 1500–1750 cm^{-1} with the addition of RR24 may be due to the formation of this quinoid structure.

3.1.2. Thermogravimetric analysis

The amount of water absorbed in the BSG is indicated by approximately 5% mass loss (endothermic) between 40 and 95°C (Figure 1(d)). Between 225 and 350°C, the mass loss of 47–48% represents the release of oils, waxes, alkaloids, glycosides, and extractive organic compounds, among other things, due to the thermal degradation of cellulose, lignin, and hemicellulose. At 500°C, it shows a significant aromatisation of the endothermic material. Similar findings have been reported by many researchers [35,38,39]. Under the conditions of the experiment, the results show that BSG particles can keep their original physical properties.

3.1.3. SEM analysis

Figure 2(a) shows that the BSG surface is heterogeneous and contains regular fibres due to its lignocellulosic content. The fibrous morphology of the BSG has not significantly

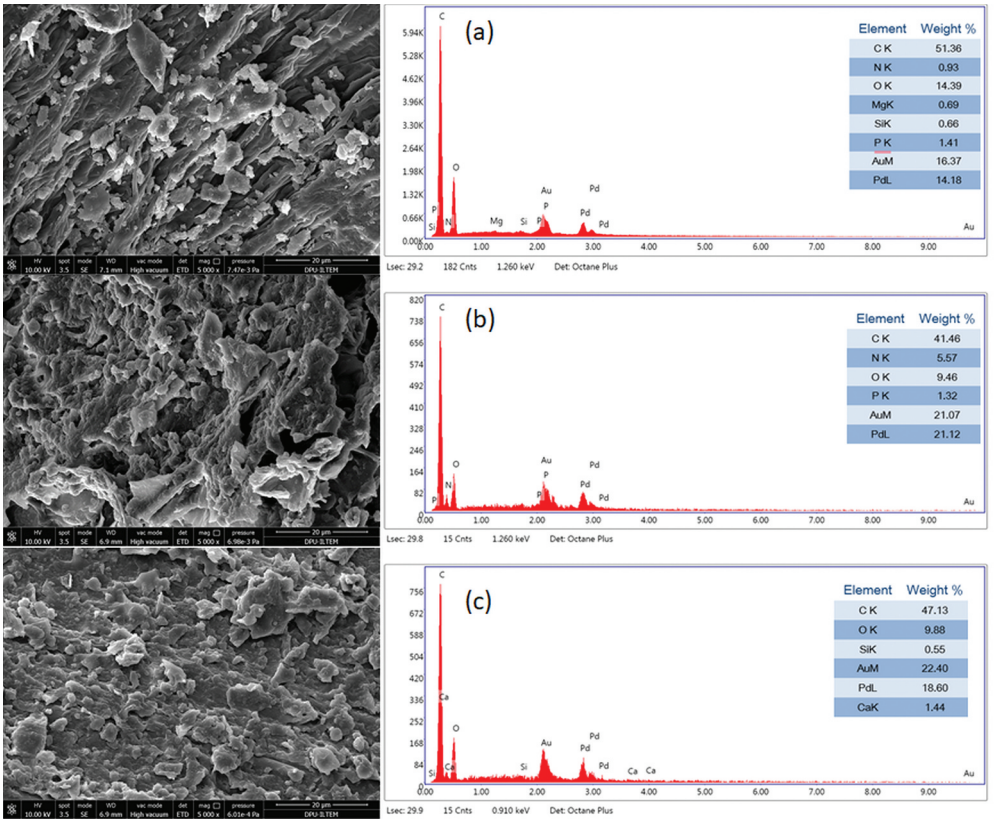

Figure 2. SEM/EDX of BSG (a), RR24 loaded BSG (b), MB loaded BSG (c).

changed following the adsorption process, but a mass of tiny particles can be accumulated on the dye-loaded BSG (Figure 2(b,c)). Furthermore, EDX analysis demonstrated that, after dye adsorption, the %C content of BSG decreased as predicted. This is because RR24 and MB have a low carbon to BSG ratio. Furthermore, the amount of %N in BSG loaded with RR24 increased from 0.93% to 5.57% in the EDX analysis. However, there was no detectable increase in nitrogen levels after MB adsorption. Differences in their chemical structures and properties may explain why RR24 has a higher affinity for binding to BSG than MB.

3.2. Effect of pH

pH is a crucial factor in the adsorption process as it determines the surface properties of adsorbents. The amount of electrostatic charge imparted by the ionised dye molecules depends on the pH of the medium. As a result, the pH of the aqueous medium will affect the adsorption rate [7]. For basic (cationic) dye adsorption, the proportion of dye removal typically decreases at low pH solutions, whereas the percentage of dye removal for reactive (anionic) dyes increases. In contrast, the proportion of dye removal will rise for cationic dye adsorption and fall for anionic dye adsorption in a high pH solution. The linear range of pH sensitivity is determined by the point of zero charges (pH_{pzc}), which also identifies the kind of active surface centres and the surface's capacity for adsorption [7,40]. Many studies have examined the pH_{pzc} of adsorbents to understand the adsorption mechanism in adsorption processes where agricultural wastes are used as adsorbents [11,41]. Because functional groups like OH^- and COO^- are present, MB adsorption is more advantageous at $pH>pH_{pzc}$. The surface becomes positively charged at $pH<pH_{pzc}$, which favours RR24 adsorption [42,43]. Figure 3(a) is illustrated how pH affects the RR24 and MB adsorption capacities of BSG, and Figure 3(b) is depicted to determine the point of zero charges (pH_{pzc}=6.0). The optimal pH value for MB adsorption on BSG was determined to be 7.00 (42.8%) and 1.50 (86.2%) for RR24 adsorption. As the equilibrium pH rises above the pH_{pzc}, the surface charge of BSG becomes negative due to deprotonation of the carboxyl groups, causing strong electrostatic attraction towards MB and preventing the aggregation of BSG particles, which limits the interaction between surface functional groups. Similarly, at low pH values, BSG's surface charge becomes more positively charged, which attracts RR24 and facilitates its adsorption. The positive surface charge enhances the electrostatic interaction between the negatively charged dyes and the positively charged surface, thereby increasing adsorption efficiency.

3.3. Effect of adsorbent dosage

It is crucial to analyse the adsorbent dosage in the adsorption process to determine cost-effectiveness. Examining the adsorption studies in the literature leads to the conclusion that the amount of adsorption has a direct relationship with the amount of adsorbent, as depicted by the diagrams based on adsorbent quantity and adsorption capacity [44]. The adsorption capacity declined when the adsorbent dose was increased beyond the optimum level, according to the results, which may have been due to the tendency of the adsorbent to aggregate or overlap with other adsorbents [45]. With an increase in adsorbent dose, the number of active sites suitable for dye adsorption increases, and so

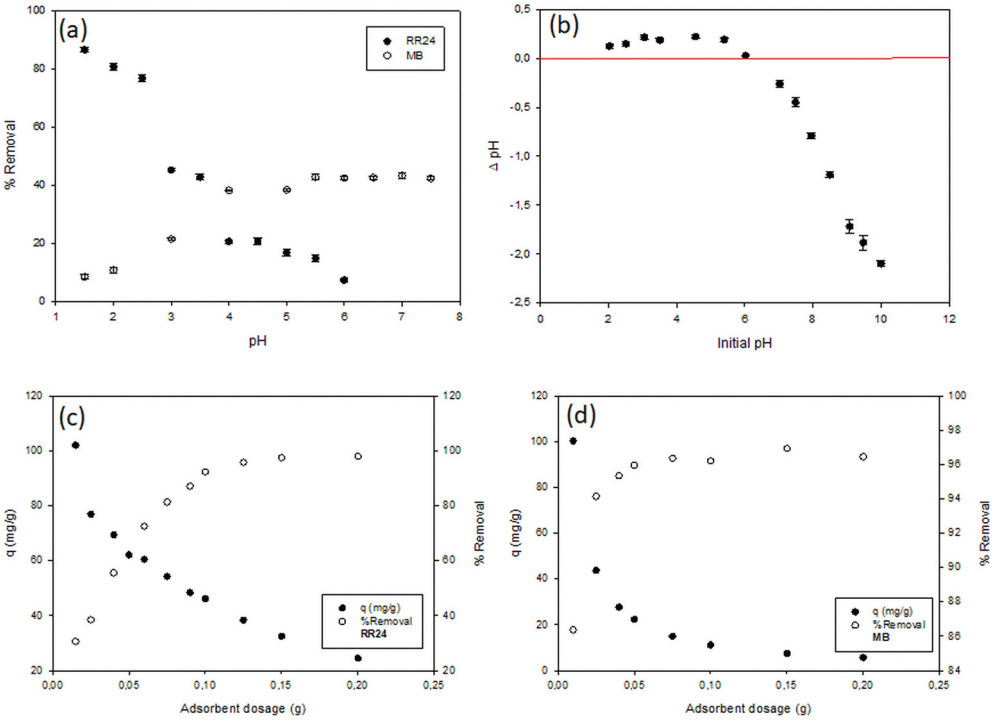

Figure 3. Effect of pH for the adsorption of RR24 and MB onto BSG at 20°C (a); determination of pH_{pzc} of BSG (b); effect of adsorbent dosage for RR24 (c) and MB(d).

does the adsorption efficiency. However, the adsorption capacity decreases as the active sites of the adsorbent remain unsaturated [46,47].

0.150 g of BSG in 50 mL of dye solution provided 32.48 mg/g (97.6 ± 0.4%) and 7.51 mg/g (96.9 ± 0.2%) dye removal for RR24 (Figure 3(c)) and MB (Figure 3(d)), respectively. The amount of adsorbent increased by 0.05 g, which led to an increase in RR24 and MB removal of about 0.5%. As a result, while the adsorbent amount was increased, the removal capacity remained constant. This is due to the adsorption reaching the saturation state. In other words, adsorption reaches saturation when the BSG tends to get saturation [11]. In the study by Jegan et al., similar results for removing cationic dye (Basic Blue 41 and Basic Blue 09) were reported [48]. Fontana et al. evaluated the effect of adsorbent dosages ranging from 0.8 to 10 g/L on dye removal efficiency. With 2.8 g/L of adsorbent, the dye was quickly adsorbed upto 96%. It was reported that increasing the amount of adsorbent beyond this value did not affect dye removal significantly [49].

3.4. Effect of temperature and contact time

Understanding how temperature affects the adsorption process is useful for determining the adsorbent's sorption capacity. Several researchers have found that an increase in temperature greatly increases the degree of diffusion of solutes, thus strongly influencing the uptake potential of adsorbents towards solutes [50,51]. Using agricultural wastes as an adsorbent in an adsorption process has a relatively

limited temperature sensitivity; that is, the effect is only slightly noticeable in the low-temperature range [52]. This is beneficial because it means that the adsorption process can take place over a wide range of temperatures, without any significant adjustment or limitation. This makes the adsorption process more efficient, since it allows the process to take place over a broader range of temperatures and doesn't require additional energy input to modify or adjust the temperature. As a result, this flexibility can allow the adsorption process to be more cost effective and less time consuming.

The adsorption capacity of RR24 and MB onto BSG as a function of contact time at various temperatures is illustrated in Figure 4(a,b) respectively. The amount of adsorbed RR24 (Figure 4(a)) increased with temperature during the first ten minutes of the adsorption process, but this effect was lost after equilibrium was reached at all temperatures. Similarly, in MB adsorption (Figure 4(b)), the temperature increase did not affect the adsorption capacity, while the adsorption process reached equilibrium within 5 min. This suggests that the adsorption of MB onto BSG is physical in nature and not greatly affected by temperature, while the RR24 removal is likely to be due to a combination of physical and chemical interactions that depend more on temperature. In addition, the findings indicate that BSG's adsorption capacity is not enhanced by sustained exposure to higher temperatures.

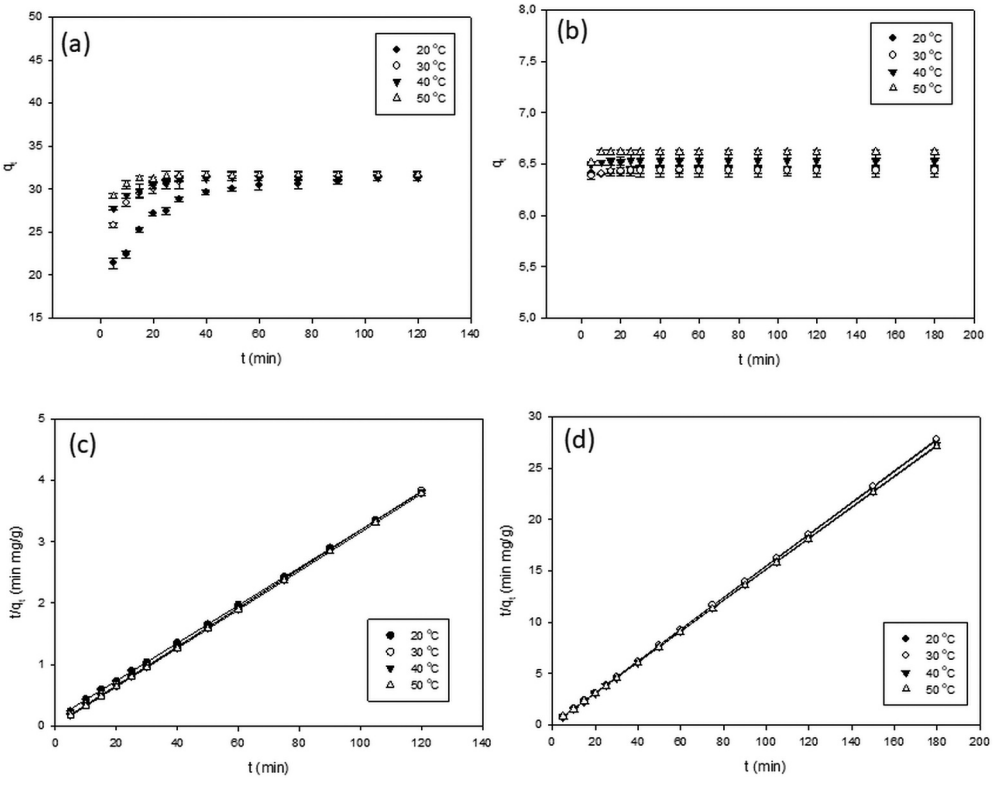

Figure 4. Effect of contact time for RR24 (a) and MB (b), Pseudo-second-order kinetic plots for the adsorption of RR24 (c) and MB (d) onto BSG at various temperatures.

3.5. Kinetics of RR24 and MB adsorption

Adsorption rate of a material is determined by its interaction rate with the target adsorbate, which depends on its surface area, porosity, and other physical and chemical properties. The adsorption rate is the rate at which the adsorbent material takes up molecules of a given adsorbate. The adsorption rate is an important consideration when selecting an adsorbent material; the adsorbent should have a high adsorption capacity and a rapid adsorption rate. Most adsorption studies have used diverse kinetic models (Pseudo-first-order, Pseudo-second-order, Elovich etc.) to investigate adsorption kinetics. The Pseudo-first-order kinetic model does not always accurately predict the amount of dye adsorbed over the entire contact time range. Therefore, it has been found in many studies that the adsorption kinetics fit the pseudo-second-order kinetic model based on the sorption capacity of the solid phase [7]. This model has been widely accepted as a reliable kinetic model for the analysis of adsorption data and elucidation of adsorption mechanisms [53–55]. In this study, the adsorption kinetics of RR24 and MB onto BSG are based on pseudo-first-order (Figure not shown) and pseudo-second-order kinetic models (Figure 4(c) for RR24, Figure 4(d) for MB). The equations of the models are given below;

Pseudo-first-order kinetic model [56]

$$\ln(q_e - q_t) = \ln q_e - k_1 t \tag{3}$$

Pseudo-second-order kinetic model [57]

$$\frac{t}{q_t} = \frac{1}{q_e^2 k_2} + \frac{1}{q_e} t \tag{4}$$

h_o, the initial sorption rate (mg/g min), was calculated according to the following equation using k_2 [58]

$$h_o = q_e^2 k_2 \tag{5}$$

where q_e (mg/g) is the amount of dye adsorbed per unit mass of the BSG at equilibrium and q_t (mg/g) is adsorption capacity at time t. k_1 (1/min) and k_2 (g/mg min) are pseudo-first-order and pseudo-second-order rate constants, respectively. All parameters calculated from the kinetic data obtained at different temperatures are given in Table 2. According to these results, the adsorption kinetics fitted pseudo-second-order kinetic model (Figure 4(c,d); $r^2 = 0.999$) moreover, the calculated q_e values at all investigated

Table 2. Kinetic parameters for RR24 and MB adsorption onto BSG.

			Pseudo-first-order			Pseudo-second-order			
	q (mg/g) experimental	t (° C)	k_1 (min^{-1})	q_1 (mg/g)	r_1^2	k_2 (g/mg min)	q_e (mg/g)	r_2^2	h_o (mg/g min)
RR24	30.90 ± 0.81	20	3.61×10^{-2}	10.4	0.965	7.76×10^{-3}	32.58	0.999	0.82×10
	31.31 ± 0.11	30	4.82×10^{-2}	1.91	0.675	3.65×10^{-2}	31.62	0.999	3.65×10
	31.18 ± 0.21	40	4.13×10^{-2}	1.81	0.759	4.90×10^{-2}	31.60	0.999	4.90×10
	30.91 ± 0.18	50	5.20×10^{-2}	0.70	0.699	1.20×10^{-1}	31.81	0.999	1.21×10^2
MB	6.47 ± 0.02	20	9.58×10^{-3}	0.030	0.314	3.20	6.49	0.999	1.35×10^2
	6.49 ± 0.11	30	8.91×10^{-3}	0.021	0.282	5.37	6.47	0.999	2.25×10^2
	6.59 ± 0.05	40	7.36×10^{-3}	0.037	0.370	3.29	6.60	0.999	1.43×10^2
	6.64 ± 0.09	50	2.82×10^{-3}	0.027	0.095	10.5	6.64	0.999	4.63×10^2

temperatures are very close to the experimentally obtained q values in equilibrium. During the adsorption process, it is crucial that kinetic models can confirm experimental data and model-predicted values [46]. While the effect of temperature was more noticeable during the initial minutes of RR24 adsorption onto BSG, and then it disappeared as the adsorption process reached the equilibrium. This indicates that RR24 adsorption is more susceptible to temperature changes during the initial stages of the process, but it becomes less sensitive as the process reaches the equilibrium. In addition, while the temperature-dependent adsorption capacity did not change in RR24 removal, the adsorption rate increased, which is also supported by the k_2 (7.76×10^{-3} g/mg min at 20°C; 1.20×10^{-1} g/mg min at 50°C) values in Table 2. Kinetic parameters demonstrate that the adsorption of RR24 by BSG is accelerated at higher temperatures, indicating the endothermic nature of the dye adsorption process [49]. Comparing the initial sorption rates, h_o, of both dyes reveals that MB adsorption (4.63×10^2 mg/g min) onto BSG is significantly faster than RR24 adsorption (8.24 mg/g min). This indicates that most MB adsorption occurs within the first five minutes due to physical adsorption and the time required to reach equilibrium.

The activation energy is the minimum kinetic energy required for a reaction to occur and is an estimate of the energetic barrier the adsorbate must overcome prior to adsorption. The activation energy can be determined by fitting k_2 to the Arrhenius equation at various temperatures [59]. Arrhenius equation for the second-order kinetics model is given as follows:

$$\ln k_2 = \ln A - \frac{E_a}{RT} \tag{6}$$

where E_a (J/mol) is the activation energy, A (g/mg min) the Arrhenius factor, R (8.314 J/K mol) the gas constant and T (K) is the solution temperature. The magnitude of activation energy demonstrates whether adsorption is predominantly physical or chemical. Lower activation energies (5–40 kJ/mol) suggest physisorption, whereas activation energies (40–800 kJ/mol) indicate chemisorption [60,61]. The magnitude of activation energy is, therefore, an important factor for understanding the adsorption process and the strength of the interaction between the adsorbent and adsorbate. The activation energy of both dye adsorptions was calculated from the slope values obtained from the $\ln k_2$ versus $1/T$ plot (Figure not shown). The activation energy for RR24 adsorption onto BSG was calculated as 67.30 kJ/mol, while it was 23.90 kJ/mol for MB adsorption. The low activation energy for MB adsorption onto BSG indicates that the process is conducted primarily by physical forces, while the higher activation energy for RR24 suggests that chemisorption is taking place for this adsorbate. Additionally, RR24 has a greater affinity for BSG than MB, with the higher activation energy indicating a stronger interaction between RR24 and BSG.

3.6. Isotherms of RR24 and MB adsorption

Adsorption isotherms represent the adsorption equilibrium. Adsorption isotherms are the relationships between the amount of substance q_e retained per unit weight of the adsorbent and the adsorbate concentration C_e remaining in the aqueous solution at a constant temperature. Adsorption isotherms provide important information for the understanding and design of processes involving in the adsorption process [62]. In

general, the capacity of an adsorbent for a specific adsorbate is determined by the interaction of three properties: the concentration of the adsorbate in the fluid phase, the concentration of the adsorbate in the solid phase, and the system temperature [63]. The overall adsorption capacity is determined by these properties, as the concentration and temperature of the system have a significant effect on the equilibrium between C_e and q_e (Figure 5(a)). The form of the equilibrium adsorption isotherm reveals the homogeneity and heterogeneity of the surface of the adsorbent [64,65]. In the present study, the RR24 and MB adsorption were analysed by Langmuir [66], Freundlich [67], and Temkin isotherm models [68].

$$Langmuir\ isotherm\ models;\ q_e = \left(\frac{q_m K_L C_e}{1 + K_L C_e}\right) \tag{7}$$

$$R_L = \left(\frac{1}{1 + K_L C_o}\right) \tag{8}$$

$$Freundlich\ isotherm\ models;\ q_e = K_F.C_e^{1/n} \tag{9}$$

$$Temkin\ isotherm\ models;\ q_e = \mathrm{B}lnA + \mathrm{B}lnC_e \tag{10}$$

where q_e and q_m (mg/g) are the equilibrium and maximum adsorption capacities and C_o and C_e (mg/L) are the initial and equilibrium concentrations of dyes, respectively. The Langmuir constant, K_L (L/mg), is temperature and adsorption enthalpy dependent; it is also known as the R_L (dimensionless) separation factor or equilibrium parameter [69]. K_F ((mg/g) $(L/mg)^{1/n}$) and n are Freundlich isotherm constants. B is the Temkin isotherm constant related to the heat of adsorption. A (L/mg) is the equilibrium binding constant corresponding to the maximum binding energy.

Data updated to the Langmuir, Temkin, and Freundlich isotherms indicate that the adsorption of the RR24 and MB dyes onto the BSG can be explained by the isotherms, as listed in Table 3. Based on the correlation coefficient (r^2), the Langmuir model explains the adsorption process better than the other models. The Langmuir isotherm (Figure 5(b)) is found to fit the data best, suggesting that the adsorption process on the BSG followed a single monolayer formation mechanism. The highest adsorption capacities for MB and

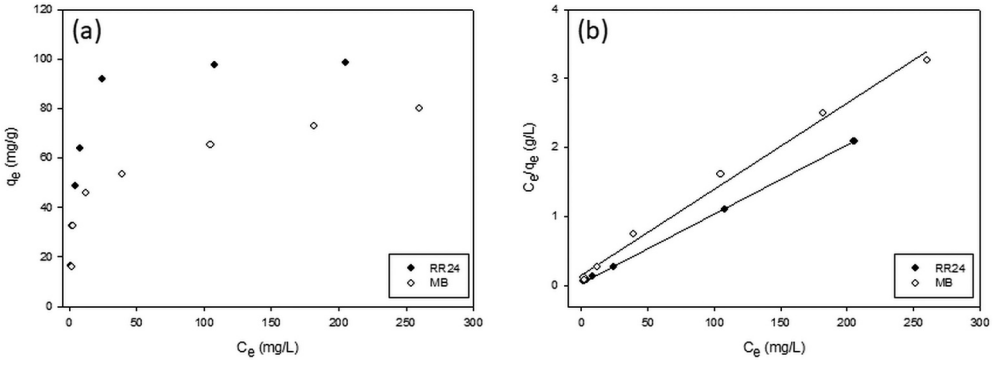

Figure 5. Adsorption isotherms of RR24 and MB (a); Langmuir isotherms of RR24 and MB (b) at 30°C.

Table 3. Isotherm parameters for MB and RR24 adsorption onto BSG.

	MB	RR24
Langmuir		
q_m (mg/g)	80.31	100.52
K_L (L/mg)	8.27×10^{-2}	2.39×10^{-1}
R_L	2.36×10^{-2}	8.28×10^{-3}
r_L^2	0.992	0.999
Freundlich		
n	3.851	3.285
K_F ((mg/g)(L/mg)$^{1/n}$)	19.83	25.55
r_F^2	0.875	0.812
Temkin		
A (L/mg)	4.24	4.61
B	10.95	15.93
r_T^2	0.960	0.921

RR24 dyes were 80.31 and 100.52 mg/g, respectively. The q_e values found to be lower than the q_m values that were calculated from the experimental data. This trend is consistent with cases reported in the literature [69,70] and suggests that adsorption occurs as a monolayer phenomenon and BSG is not completely covered by the dyes. Analyzing the R_L constant values of RR24 and MB (8.28×10^{-3} and 2.36×10^{-2}), it was determined that the adsorption process was favourable. This finding is supported by the values of $n \geq 1$ (Freundlich constant) for both of the dyes. The steep initial slope of adsorption isotherm is attributed to low K_L values, indicating an ideally high affinity. According to Kratochvil and Volesky, a favourable adsorbent should have a low Langmuir constant K_L and a high q_m value [70,71]. The K_L values found for RR24 and MB dyes in this study were 8.27×10^{-2} and 2.39×10^{-1} L/mg, respectively; the q_m values are 100.52 and 80.31 mg/g. In the study of malachite green and congo red adsorption onto BSG carried out by Chanzu et al., the K_L values were 1.55 and 0.0189 L/mg, and the q_m values were 2.55 and 36.5 mg/g, respectively [72]. The dye adsorption capacities of BSG is comparable with the literature. For example, the adsorption capacity of Orange D-TGL [49] was 23.20 mg/g; Blue BF-5 G was 42.58 mg/g [11], and Tartrazine yellow was 26.18 mg/g [38]. In the literature, the q_m for RR24 adsorption on rice husk biochar was reported to be 88.51 mg/g [73], whereas Azolla pinnata [74] and sugarcane bagasse [75] had maximum adsorption capacities of 80.6 and 9.41 mg/g for MB adsorption, respectively. The study shows that BSG used as an adsorbent is a promising adsorbent in the removal of reactive and basic dyes, even though it has not been used without any prior treatment. Further research needs to be conducted to fully understand the potential of BSG and its effectiveness in dye removal.

3.7. Adsorption mechanism

Agricultural waste surfaces, which are primarily composed of lignin, cellulose, and hemicellulose, contain hydroxyl, methoxyl, and carbonyl groups [53]. Mechanisms for molecular binding in dyestuffs rely heavily on these functional groups. The Arrhenius equation yields E_a values of 67.30 kJ/mol for RR24 adsorption and 23.90 kJ/mol for MB adsorption. Positive E_a values indicate that an endothermic process facilitates the adsorption of both dyes; additionally, the removal of RR24 is chemisorption, while the removal of MB is physisorption. The RR24 structure's chlorine is very likely to form covalent bonds with the hydroxyl and carboxyl groups on the

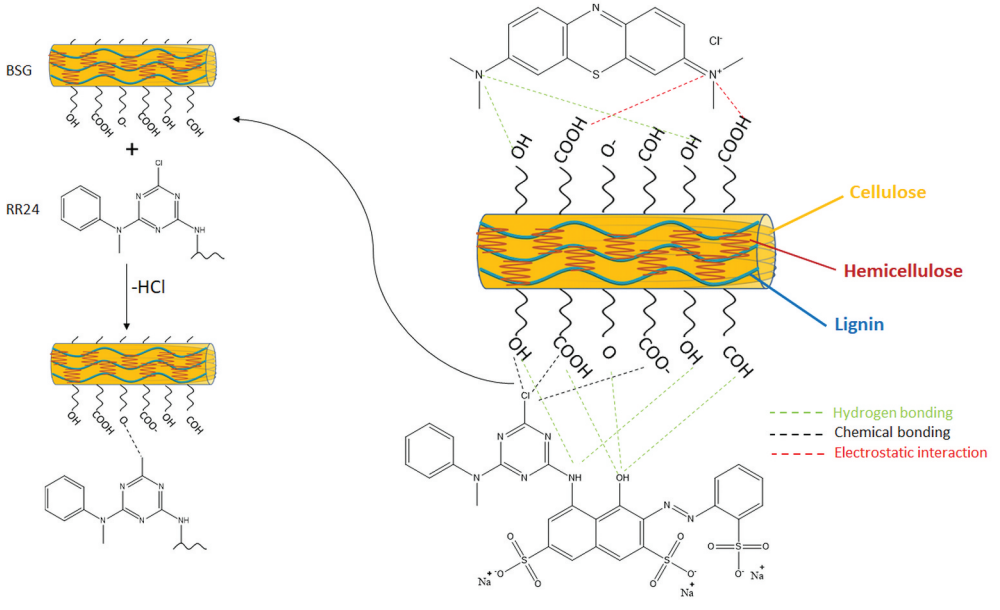

Figure 6. Proposed adsorption mechanisms between BSG surface and RR24/MB dyes.

BSG surface due to its oxidising, highly active, and prone to nucleophilic substitution nature. Furthermore, the adsorption process involves the formation of hydrogen bonds between the -NH groups in both dyes and the -OH groups on the BSG surface (Figure 6). Another interaction that could be expected to occur during MB adsorption is the electrostatic attraction between $-NH_2^+$ and $-COO^-$ [38]. As a result, the mechanisms and dyes used caused differences in the adsorption capacity of BSG.

3.8. Effect of ionic strength

In general, wastewater from industries that produce dyes contains not only dyes but also several other compounds that should be taken into account during dye adsorption. The presence of high ion concentrations produces wastewater with a high ionic strength, which may interfere with the dye adsorption process [49,76]. Ionic strength was adjusted using KCl at various concentrations (0.02–0.6 M). At room temperature, the effect of ionic strength on the adsorption of RR24 and MB onto BSG was evaluated using various concentrations of KCl. Figure 7(a,b) depicts the effect of KCl concentration on the adsorption process. The adsorption removal of RR24 and MB on BSG without salt is $97.58 \pm 0.58\%$ and $96.45 \pm 0.61\%$, respectively. Increasing the salt concentration as the KCl concentration varies from 0.01 to 0.6 mol/L, the removal percentage decreases slightly. RR24 and MB removals decreased to $88.10 \pm 0.37\%$ and $85.20 \pm 0.51\%$, respectively, in the presence of 0.6 mol/L KCl. This is likely due to the decreased number of charged surface sites that are required for RR24 and MB to adhere, as the presence of KCl reduced the availability of these sites. It is therefore possible that electrostatic interactions are a significant factor in dye adsorption on BSG.

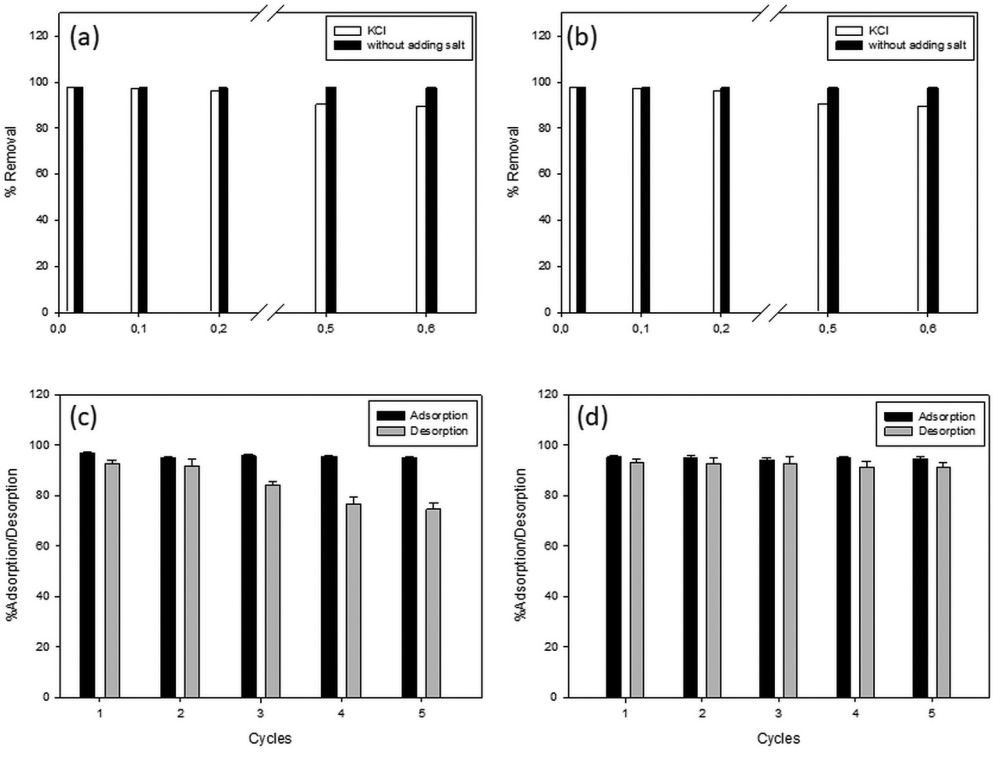

Figure 7. Effect of ionic strength for RR24 (a) and MB (b); adsorption/desorption studies of RR24 (c) and MB (d).

3.9. Desorption studies

15.0 mL of a 100 mg/L RR24/MB solution was combined with 45 mg of BSG at the appropriate pH. The remaining amount of dye in the solution was determined by centrifuging the solution. For RR24, 0.1 M NaOH solution was used to remove the dye from the adsorbent, while 0.1 M HCl solution was used for MB. To remove the dyes RR24 and MB from the adsorbent 0.1 M NaOH and 0.1 M HCl solutions were used respectively. Five adsorption-desorption cycles were performed on BSG to determine the reusability of the adsorbent. Figure 7(c,d) depicts the results obtained by the regeneration experiment. The adsorption values for RR24 did not change significantly between the first and fifth cycles (96.81–94.90%), while the desorption amounts decreased from 92.68% to 74.90%. On the other hand, neither adsorption (95.35–94.72%) nor desorption (93.25–91.28%) amounts for MB changed significantly between the first and fifth cycles. This suggests that the positively charged surface effectively attracts and retains the reactive dyes, resulting in high adsorption efficiency. However, the desorption amounts for RR24 decreased significantly over the cycles, indicating that it may be more challenging to remove from the surface than MB. According to these results, it can be proposed that the operating cost of the adsorption can be reduced by the help of this effective regeneration process. In Figure 7(c,d), it is seen that the adsorption efficiencies of both dyes remained almost constant. In addition, MB dyestuff was recovered in all cycles. In the RR24 adsorption

cycles, the desorption efficiency decreased in the fourth and fifth cycles. This supports the conclusion that the RR24 dyestuff binds to the BSG surface by chemisorption and physisorption. These findings suggest the effective reusability of BSG for at least three cycles for RR24 and five cycles for MB removal.

3.10. Studies of synthetic wastewater

Synthetic wastewater mimics real-life conditions and allows researchers to accurately study the behaviour of reactive and basic dyes when interacting with BSG. By adding both organic and inorganic materials to the experiments, important information can be learned about how well BSG works as an adsorbent in complex wastewater treatment scenarios. These insights can help in optimising the use of BSG in large-scale wastewater treatment plants where various contaminants are present. Additionally, studying the behaviour of reactive and basic dyes with BSG in synthetic wastewater can aid in developing efficient and cost-effective treatment methods for industrial effluents containing these dyes. Under optimal adsorption conditions, experiments were conducted to evaluate the BSG's potential performance in removing RR24 and MB from synthetic wastewater. At 20°C, 0.150 g of BSG was added to the dye solution, which had already been brought to the optimum pH for both dyes. RR24 and MB removal from synthetic wastewater were found to be 95.81 ± 0.44% and 95.33 ± 0.30%, respectively. The results clearly demonstrated that there was no significant matrix effect on the effective removal of RR24 and MB from wastewater. Due to its high adsorption performance, BSG that has not been pre-treated can also treat wastewater with reactive and basic dyes.

4. Conclusion

Brewer's Spent Grain (BSG), which has the highest waste rate among brewery wastes, was used as an adsorbent in the study without any pre-treatment. Here, it aims to determine the cleaning ability of wastewater with factory wastes and conduct preliminary research to enhance the adsorption capacity. In addition, the adsorption processes of reactive (RR24) and basic (MB) dyes on BSG were investigated depending on pH, time, amount of adsorbent, and temperature.

For RR24 adsorption on BSG, the maximum adsorption amount was reached at pH = 1.50, whereas for MB adsorption, it was reached at pH = 7.00. The dosage of adsorbent for both dyes was determined to be 0.150 g. In adsorption experiments conducted at various temperatures, it was observed that the MB adsorption reached equilibrium in a short period of time, approximately 5 minutes and that the temperature had no effect on the adsorption process. Also, it was discovered that the rate of RR24 adsorption increased with temperature, whereas the adsorption capacity remained relatively unchanged. The activation energies of RR24 and MB adsorption were 67.3 and 23.9 kJ/mol, respectively. These findings indicate that MB adsorption on BSG is physisorption, whereas RR24 adsorption is chemisorption. The adsorption of both dyestuffs was consistent with the pseudo-second-order kinetic model for all temperatures studied. In addition, it was found that the Langmuir isotherm model could best explain the adsorption of MB and RR24, and the maximum adsorption capacities were 80.31 and 100.52 mg/g, respectively. Compared

with the literature, the dye adsorption capacity of BSG is entirely satisfactory. Furthermore, BSG's removal efficiency, low cost, and being able to be used without pre-treatment show that it is a promising adsorbent, an agricultural waste. Future research could increase the adsorption capacity by increasing the number of functional groups on the BSG surface.

Acknowledgments

The authors wish to thank Anadolu Efes Brewing and Malt Industry in Kahramanankazan/Turkey for providing the used brewers' spent grain.

Disclosure statement

No potential conflict of interest was reported by the author(s).

Funding

This research was supported by the Kütahya Dumlupınar University Scientific Research Projects Coordination Office [Project No: 2022-40].

ORCID

Çiğdem Ay http://orcid.org/0000-0002-8283-0678
Şaziye Betül Sopaci http://orcid.org/0000-0002-2840-4985
Orhan Atakol http://orcid.org/0000-0003-0977-6588
Sevi Öz http://orcid.org/0000-0002-4628-0365

References

[1] A. Azari, R. Nabizadeh, S. Nasseri, A.H. Mahvi and A.R. Mesdaghinia, Chemosphere **250**, 126238 (2020). doi:10.1016/j.chemosphere.2020.126238.
[2] B.J. Brüschweiler and C. Merlot, Regul. Toxicol. Pharmacol. **88**, 214–226 (2017). doi:10.1016/j.yrtph.2017.06.012.
[3] A.K.M. Atique Ullah, A.K.M. Fazle Kibria, M. Akter, M.N.I. Khan, A.R.M. Tareq and S.H. Firoz, Water Conserv. Sci. Eng. **1**, 249–256 (2017). doi:10.1007/s41101-017-0017-3.
[4] M.S. Reisch, Chem. Eng. News Arch. **74**, 10–12 (1996). doi:10.1021/cen-v074n052.p010.
[5] N. Tara, S.I. Siddiqui, G. Rathi, S.A. Chaudhry, Inamuddin and A.M. Asiri, Curr. Anal. Chem. **16** (1), 14–40 (2020). doi:10.2174/1573411015666190117124344.
[6] F. Ayachi, E.C. Lima, A. Sakly, H. Mejri and A. Ben Lamine, Prog. Biophys. Mol. Biol. **141**, 47–59 (2019). doi:10.1016/j.pbiomolbio.2018.07.004.
[7] M.A.M. Salleh, D.K. Mahmoud, W.A.W.A. Karim and A. Idris, Desalination **280** (1–3), 1–13 (2011). doi:10.1016/j.desal.2011.07.019.
[8] S. Iranfar, M. Hekmati, H. Ziyadi, E. Ghasemi and D. Esmaeili, Inorg. Chem. Commun. **133** (September), 108925 (2021). doi:10.1016/j.inoche.2021.108925.
[9] R. Malik, D.S. Ramteke and S.R. Wate, Waste Manag. **27** (9), 1129–1138 (2007). doi:10.1016/j.wasman.2006.06.009.
[10] S. Rangabhashiyam, N. Anu and N. Selvaraju, J. Environ. Chem. Eng. **1**, 629–641 (2013). doi:10.1016/j.jece.2013.07.014.

[11] P.T. Juchen, H.H. Piffer, M.T. Veit, G. Da Cunha Gonçalves, S.M. Palácio and J.C. Zanette, J. Environ. Chem. Eng. **6**, 7111–7118 (2018). doi:10.1016/j.jece.2018.11.009.
[12] F. Ezbakhe, J. Water Pollut. Control **1** (1), 6 (2018). https://www.imedpub.com/articles/addressing-water-pollution-as-a-means-to-achieving-the-sustainable-development-goals.php?aid=22766.
[13] J. Smet and C. Van Wijk, *Small Community Water Supplies Technology, People and Partnership* (IRC International Water And Sanitation, Centre, Netherlands, 2002).
[14] UNICEF, *United Nations Children's Fund (UNICEF) Handbook on Water Quality* (New York, USA, 2008).
[15] N.B. Aruna, A.K. Sharma and S. Kumar, Chemosphere **268**, 129309 (2021). doi:10.1016/j.chemosphere.2020.129309.
[16] A. Bhatnagar and M. Sillanpää, Chem Eng. J. **157**, 277–296 (2010). doi:10.1016/j.cej.2010.01.007.
[17] A.M. Elgarahy, K.Z. Elwakeel, S.H. Mohammad and G.A. Elshoubaky, Clean. Eng. Technol. **4**, 100209 (2021). doi:10.1016/j.clet.2021.100209.
[18] D.A. Giannakoudakis, A. Hosseini-Bandegharaei, P. Tsafrakidou, K.S. Triantafyllidis, M. Kornaros and I. Anastopoulos, J. Environ. Manage. **227**, 354–364 (2018). doi:10.1016/j.jenvman.2018.08.064.
[19] A. Kumar and H. Gupta, Environ. Technol. Innov. **20**, 101080 (2020). doi:10.1016/j.eti.2020.101080.
[20] G.L. Dotto and G. McKay, J. Environ. Chem. Eng. **8**, 103988 (2020). doi:10.1016/J.JECE.2020.103988.
[21] P.S. Thue, M.A. Adebayo, E.C. Lima, J.M. Sieliechi, F.M. Machado, G.L. Dotto, J.C.P. Vaghetti and S.L.P. Dias, J. Mol. Liq. **223**, 1067–1080 (2016). doi:10.1016/J.MOLLIQ.2016.09.032.
[22] M.A. Zazycki, M. Godinho, D. Perondi, E.L. Foletto, G.C. Collazzo and G.L. Dotto, J. Clean. Prod. **171**, 57–65 (2018). doi:10.1016/J.JCLEPRO.2017.10.007.
[23] A. Thanarasu, K. Periyasamy, P. Manickam Periyaraman, T. Devaraj, K. Velayutham and S. Subramanian, Mater. Today Proc. **36**, 775–781 (2019). doi:10.1016/j.matpr.2020.07.001.
[24] S. Wang and Z.H. Zhu, J. Hazard. Mater. **136**, 946–952 (2006). doi:10.1016/j.jhazmat.2006.01.038.
[25] N.A.H. Mohamad Zaidi, F.N. Sallehuddin, L.B.L. Lim and M.R.R. Kooh, Int. J. Environ. Anal. Chem. **103**, 1836–1854 (2021). doi:10.1080/03067319.2021.1884238.
[26] A. Es-Said, H. Nafai, G. Lamzougui, A. Bouhaouss and R. Bchitou, Sci. Afr. **13**, e00960 (2021). doi:10.1016/J.SCIAF.2021.E00960.
[27] B. Liu, C. Du, J.J. Chen, J.Y. Zhai, Y. Wang and H.L. Li, Chem. Phys. Lett. **771**, 138535 (2021). doi:10.1016/J.CPLETT.2021.138535.
[28] TEPGE, *Product Search Report: Barley* (T.R. Ministry Of Agriculture And Forestry, 2022).
[29] K. Rachwał, A. Waśko, K. Gustaw and M. Polak-Berecka, PeerJ **8**, 1–28 (2020). doi:10.7717/peerj.9427.
[30] S.I. Mussatto, G. Dragone and I.C. Roberto, J. Cereal Sci. **43**, 1–14 (2006). doi:10.1016/J.JCS.2005.06.001.
[31] Y. Su, M. Wenzel, S. Paasch, M. Seifert, W. Böhm, T. Doert and J.J. Weigand, ACS Omega **6** (30), 19364–19377 (2021). doi:10.1021/acsomega.1c00589.
[32] M. Roth, M. Jekle and T. Becker, Trends Food Sci. Technol. **91**, 282–293 (2019). doi:10.1016/J.TIFS.2019.07.041.
[33] B. Nadolny, R.G. Heineck, H.A.G. Bazani, J.V. Hemmer, M.L. Biavatti, C.M. Radetski and G. I. Almerindo, J. Environ. Sci. Heal. Part A. **55** (8), 947–956 (2020). doi:10.1080/10934529.2020.1759320.
[34] P. Atalay, N.A. Perendeci and M.Y. Goksungur, J. Eng. Sci. **26** (7), 1257–1266 (2020). doi:10.5505/pajes.2019.80850.
[35] Y. Su, M. Wenzel, S. Paasch, M. Acker, T. Doert, E. Brunner, T. Henle and J.J. Weigand, RSC Adv. **10**, 45116 (2020). doi:10.1039/d0ra08164g.
[36] J.S. Noh and J.A. Schwarz, J. Colloid Interface Sci. **130**, 157–164 (1989). doi:10.1016/0021-9797(89)90086-6.
[37] Ç. Ömeroğlu Ay, A.S. Özcan, Y. Erdoğan and A. Özcan, Colloids Surf. B. **100**, 197–204 (2012). doi:10.1016/j.colsurfb.2012.05.013.
[38] T.P. de Araújo, F.D.O. Tavares, D.T. Vareschini and M.A.S.D. Barros, Environ. Technol. (United Kingdom) **42** (19), 2925–2940 (2021). doi:10.1080/09593330.2020.1718217.

[39] L.E.N. Castro and L.M.S. Colpini, Eur. Food Res. Technol. **247** (12), 3013–3021 (2021). doi:10.1007/s00217-021-03860-5.
[40] A.A. Poghossian, Sens. Actuators B. **44**, 551–553 (1997). doi:10.1016/S0925-4005(97)00156-1.
[41] E. Contreras, L. Sepúlveda and C. Palma, Int. J. Chem. Eng. **2012**, 1–9 (2012). doi:10.1155/2012/679352.
[42] L.R. Radovic, I.F. Silva, J.I. Ume, J.A. Menéndez, C.A. Leon Y Leon and A.W. Scaroni, Carbon N. Y. **35** (9), 1339–1348 (1997). doi:10.1016/S0008-6223(97)00072-9.
[43] D. Savova, N. Petrov, M.F. Yardim, E. Ekinci, T. Budinova, M. Razvigorova and V. Minkova, Carbon N. Y. **41**, 1897–1903 (2003). doi:10.1016/S0008-6223(03)00179-9.
[44] A.A. Beni and A. Esmaeili, Environ. Technol. Innov. **17**, 100503 (2020). doi:10.1016/j.eti.2019.100503.
[45] E. Nakkeeran, S. Rangabhashiyam, M.S. Giri Nandagopal and N. Selvaraju, Desalin. Water Treat. **57**, 23951–23964 (2016). doi:10.1080/19443994.2015.1137497.
[46] T.A. Aragaw, Heliyon **7**, e07281 (2021). doi:10.1016/j.heliyon.2021.e07281.
[47] A. Verma, S. Kumar and S. Kumar, J. Environ. Chem. Eng. **4**, 4587–4599 (2016). doi:10.1016/J.JECE.2016.10.026.
[48] J. Jegan, S. Praveen, T. Bhagavathi Pushpa and R. Gokulan, Appl. Ecol. Environ. Res. **18** (1), 1925–1939 (2020). doi:10.15666/aeer/1801_19251939.
[49] K.B. Fontana, E.S. Chaves, J.D.S. Sanchez, E.R.L.R. Watanabe, J.M.T.A. Pietrobelli and G.G. Lenzi, Ecotoxicol. Environ. Saf. **124**, 329–336 (2016). doi:10.1016/j.ecoenv.2015.11.012.
[50] P. Saravanan, J. Josephraj and B. Pushpa Thillainayagam, Environ. Nanotechnol. Monit. Manag. **16**, 100560 (2021). doi:10.1016/J.ENMM.2021.100560.
[51] G.B. Kankiliç, A.Ü. Metin and I. Tüzün, Ecol. Eng. **86**, 85–94 (2016). doi:10.1016/J.ECOLENG.2015.10.024.
[52] I. Kim, M. Saif Ur Rehman and J.I. Han, J. Clean. Prod. **66**, 555–561 (2014). doi:10.1016/J.JCLEPRO.2013.11.072.
[53] R. Bushra, S. Mohamad, Y. Alias, Y. Jin and M. Ahmad, Microporous Mesoporous Mater. **319** (December 2020), 111040 (2021). doi:10.1016/j.micromeso.2021.111040.
[54] S. Mishra, L. Cheng and A. Maiti, J. Environ. Chem. Eng. **9**, 104901 (2021). doi:10.1016/j.jece.2020.104901.
[55] C. Bhattacharjee, S. Dutta and V.K. Saxena, Environ. Adv. **2** (September), 100007 (2020). doi:10.1016/j.envadv.2020.100007.
[56] S. Lagergren and K. Sven, Vetenskapsakademiens Handl. **24**, 1–39 (1898).
[57] Y. Ho and G. McKay, Process Biochem. **34**, 451–465 (1999). doi:10.1016/S0032-9592(98)00112-5.
[58] Z.Y. Yao, J.H. Qi and L.H. Wang, J. Hazard. Mater. **174** (1–3), 137–143 (2010). doi:10.1016/j.jhazmat.2009.09.027.
[59] Z. Aksu and S. Tezer, Process Biochem. **40**, 1347–1361 (2005). doi:10.1016/j.procbio.2004.06.007.
[60] H. Nollet, M. Roels, P. Lutgen, P. Van der Meeren and W. Verstraete, Chemosphere **53**, 655–665 (2003). doi:10.1016/S0045-6535(03)00517-4.
[61] E. Soto-Regalado, M. Loredo-Cancino, F.C. Cerino-Córdova, S. Pioquinto-Garcia and N. E. Dávila-Guzmán, Int. J. Environ. Anal. Chem. (Published online 08 May). 1–20 (2023). doi:10.1080/03067319.2023.2206025.
[62] E.N. El Qada, S.J. Allen and G.M. Walker, Chem. Eng. J. **124**, 103–110 (2006). doi:10.1016/j.cej.2006.08.015.
[63] J.F. Richardson, J.H. Harker and J.R. Backhurst, *Chemical Engineering*, 5th ed. (Elsevier, Butterworth-Heinemann, Oxford, 2002).
[64] B. Al-Duri and Y.P. Yong, Biochem. Eng. J. **4**, 207–215 (2000). doi:10.1016/S1369-703X(99)00050-9.
[65] W. Norde, Adv. Colloid Interface Sci. **25**, 267–340 (1986). doi:10.1016/0001-8686(86)80012-4.
[66] I. Langmuir, J. Am. Chem. Soc. **40**, 1361–1403 (1918). doi:10.1021/ja02242a004.
[67] H. Freundlich, Über Die Adsorpt. Lösungen. **57U**, 385–470 (1906). doi:10.1515/zpch-1907-5723.
[68] J.M. Temkin and V. Pyzhev, Acta Physicochim U.R.S.S. **12**, 327–356 (1940).
[69] K.R. Hall, L.C. Eagleton, A. Acrivos and T. Vermeulen, Ind. Eng. Chem. Fundam. **5** (2), 212–223 (1966). doi:10.1021/i160018a011.

[70] O.S. Lawal, A.R. Sanni, I.A. Ajayi and O.O. Rabiu, J. Hazard. Mater. **177**, 829–835 (2010). doi:10.1016/j.jhazmat.2009.12.108.
[71] D. Kratochvil and B. Volesky, Trends Biotechnol. **16** (7), 291–300 (1998). doi:10.1016/S0167-7799(98)01218-9.
[72] H.A. Chanzu, J.M. Onyari and P.M. Shiundu, J. Hazard. Mater. **380**, 120897 (2019). doi:10.1016/j.jhazmat.2019.120897.
[73] Y. Yang, T.M.P. Nguyen, H.T. Van, Q.T. Nguyen, T.H. Nguyen, T.B. Lien Nguyen, L.P. Hoang, D. Van Thanh, T.V. Nguyen, V.Q. Nguyen, P.Q. Thang, M. Yılmaz and V.G. Le, Mater. Sci. Semicond. Process **150**, 106960 (2022). doi:10.1016/j.mssp.2022.106960.
[74] M.R.R. Kooh, R. Thotagamuge, Y.F. Chou Chau, A.H. Mahadi and C.M. Lim, J. Taiwan Inst. Chem. Eng. **132**, 104134 (2022). doi:10.1016/j.jtice.2021.11.001.
[75] T.C. Andrade Siqueira, I. Zanette da Silva, A.J. Rubio, R. Bergamasco, F. Gasparotto, E. Aparecida de Souza Paccola and N. Ueda Yamaguchi, Int. J. Environ. Res. **17** (2), 526 (2020). doi:10.3390/ijerph17020526.
[76] N.S. Maurya, A.K. Mittal, P. Cornel and E. Rother, Bioresour. Technol. **97** (3), 512–521 (2006). doi:10.1016/j.biortech.2005.02.045.